A Multiscale Investigation of Strain Localization in Cohesionless Sand

Ning Guo and Jidong Zhao

Abstract We develop a hybrid finite-discrete element method (FEM/DEM) multiscale framework to model strain localization in cohesionless sand. This framework takes advantage of a hierarchical solution structure based on the two numerical techniques, by modeling the material as a continuum at large using FEM and deriving the material point response of the FEM mesh from a DEM assembly attached to each integration point. In doing so, the phenomenological assumptions on the macroscopic constitutive law in conventional continuum modeling can be naturally bypassed. We demonstrate the predictive capability of the model by simulating a biaxial compression test on sand where strain localization is observed. The influences of different boundary conditions on the shear band pattern are examined.

1 Introduction

Strain localization is one of the major failure mechanisms for granular materials and is considered as a precursor of many catastrophic geo-hazards in civil engineering such as slope instability, debris flow and failure of foundation. Modeling of strain localization has been an active area for both engineers and theorists using either continuum-based methods such as finite element method (FEM) (Gao and Zhao 2013; Tejchman and Wu 2009) or discrete element method (DEM) (Fu and Dafalias 2011; Ishihara and Oda 1998). However, the phenomenon of strain localization in granular media is still not well understood due partially to the two facts: First, the continuum-based methods neglect the discrete nature of granular media

N. Guo (✉) · J. Zhao
Department of Civil and Environmental Engineering, The Hong Kong University of Science and Technology, Clear Water Bay, Kowloon, Hong Kong
e-mail: ceguo@ust.hk

J. Zhao
e-mail: jzhao@ust.hk

© Springer International Publishing Switzerland 2015

K.-T. Chau and J. Zhao (eds.), *Bifurcation and Degradation of Geomaterials in the New Millennium*, Springer Series in Geomechanics and Geoengineering,
DOI 10.1007/978-3-319-13506-9_18

while the macroscopic response of the material is indeed encoded in its microscopic structural character, which makes the continuum-based method inept to explain the underlying mechanism for the macroscopic observations and being frequently criticized as phenomenological. Second, strain localization is indeed a boundary value problem (BVP) even for a sample in laboratory test, which typically involves large number of particles which cannot be effectively handled by most discrete methods due to computational cost. To address these issues, herein we present a hybrid method to study strain localization in granular media, aiming to retain the advantages of both FEM and DEM and meantime to avoid their respective limits as mentioned.

In the hybrid FEM/DEM model, the two methods are coupled in a hierarchical manner where FEM is used to solve the global BVP and a DEM assembly is attached at each Gauss integration point of the FEM mesh serving as representative volume element (RVE) (see our previous work, Guo and Zhao 2013). The local material responses are captured by the embedded DEM simulations and are provided for global solution by the FEM, while the FEM provides displacement/strain conditions as boundary conditions for each DEM at each time step. In so doing, the phenomenological nature in conventional constitutive modeling can be totally bypassed, whilst the computational efficiency of FEM in solving BVPs is retained. More importantly, the framework provides microscopic insights at the particle level thanks to the local DEM simulations, which can potentially shed lights on important physical mechanisms accounting for some macroscopic observations including the initiation and development of strain localization. The predictive capability of the hybrid multiscale framework is demonstrated by a simulation on biaxial compression tests, where different strain localization patterns are observed when an initially uniform specimen is subjected to different boundary conditions.

2 Approach

2.1 Formulations

The hybrid model is implemented by coupling two open-source codes—Escript (Gross et al. 2007) and YADE (Šmilauer et al. 2010), for FEM and DEM computations respectively. The entire problem domain is first discretized into a proper FEM mesh. The FEM solution procedure follows the conventional displacement driven formulation in solving the global weak-form governing equation for quasi-static loading in the absence of body force. For a typical nonlinear problem as in dealing with granular media, Newton-Raphson iterative method is usually adopted to solve the nonlinear equation system which requires the tangent operator $\boldsymbol{D}$ to assemble the tangent matrix. Different from the conventional FEM solution procedure where $\boldsymbol{D}$ is derived from an ad hoc constitutive assumption (e.g. the elasto-plastic modulus), the current hybrid FEM/DEM model obtains the tangent operators from the embedded discrete element assemblies.

We estimate the tangent operator from the elastic modulus $\mathbb{D}$ of a DEM packing, which can be analytically derived based on the assumption of uniform strain field (Kruyt and Rothenburg 1998):

$$\mathbb{D} = \frac{1}{V} \sum_{N_c} \left(k_n \boldsymbol{n}^c \otimes \boldsymbol{d}^c \otimes \boldsymbol{n}^c \otimes \boldsymbol{d}^c + k_t \boldsymbol{t}^c \otimes \boldsymbol{d}^c \otimes \boldsymbol{t}^c \otimes \boldsymbol{d}^c \right) \tag{1}$$

where V is the total volume of the DEM assembly, N_c is the number of contacts in the volume, k_n and k_t are the normal and tangential contact stiffnesses, $\boldsymbol{n}^c$ and $\boldsymbol{t}^c$ are the unit vectors in the outward normal and tangential directions at a contact, respectively. $\boldsymbol{d}^c$ is the branch vector connecting the centroids of the two contacted particles. This tangent operator is then used to assemble the tangent matrix for the FEM solver.

Besides the tangent operator, the stress tensor is also homogenized from the DEM packing following the Love's formula $\boldsymbol{\sigma} = \sum_{N_c} \boldsymbol{d}^c \otimes \boldsymbol{f}^c / V$ where $\boldsymbol{f}^c$ is the contact force. For 2D case, the mean and deviatoric stress can be calculated $p = \mathrm{tr}\,\boldsymbol{\sigma}/2$, $q = \sqrt{\boldsymbol{s} : \boldsymbol{s}/2}$ ($\boldsymbol{s} = \boldsymbol{\sigma} - p\boldsymbol{\delta}$). Similarly for the local strain measure, we take the symmetric part of the DEM deformation $\nabla \boldsymbol{u}$ (the anti-symmetric part accounts for rigid body rotation) $\boldsymbol{\varepsilon} = (\nabla \boldsymbol{u} + \nabla \boldsymbol{u}^T)/2$.

2.2 DEM Model and RVE Calibration

We use a linear contact law in the DEM and the Coulomb's friction criterion to describe the frictional behavior at each interparticle contact. Three input parameters are required for DEM model: the Young's modulus E_c, Poisson's ratio ν_c and the friction angle φ. The normal and tangential stiffnesses are determined by $k_n = E_c r$ and $k_t = \nu_c k_n$ where $r = 2r_1 r_2/(r_1 + r_2)$ is the common radius of the two contacted particles. A threshold for the tangential force is imposed by the friction angle such that $|f_t^c| \le f_n^c \tan\varphi$. Note that k_n and k_t will be used in Eq. (1) to calculate the tangent operator. A simple local non-viscous damping force is also added to dissipate kinetic energy $\boldsymbol{f}^{damp} = -\alpha f^{resid} \boldsymbol{v}/v$ where α is the damping ratio, $\boldsymbol{f}^{resid}$ is the residual force (unbalanced force) on the particle, $\boldsymbol{v}/v$ returns the direction of the particle velocity. All the parameters relevant to the DEM model are summarized in Table 1.

After careful calibration, we determine to use a RVE containing 400 circular disks with a particle size distribution (PSD) ranging from 3 to 7 mm such that its mechanical response is in qualitative agreement with laboratory tests on sand. The gravity force is not considered in the DEM model and periodic boundary is used in both directions of the RVE. Initially, the RVE is isotropically consolidated to a mean pressure $p_0 = 100$ kPa with an initial void ratio of 0.177.

Table 1 Parameters for the DEM model

Radii (mm)	Density (kg/m^3)	E_c (MPa)	ν_c	φ (rad)	α
3 ~ 7	2,650	600	0.8	0.5	0.1

Fig. 1 FEM mesh and boundary conditions for the biaxial compression tests. *Left* smooth boundary case; *right* rough boundary case. *Top left* 8-node 4-integration point serendipity element used for the FEM mesh in both cases

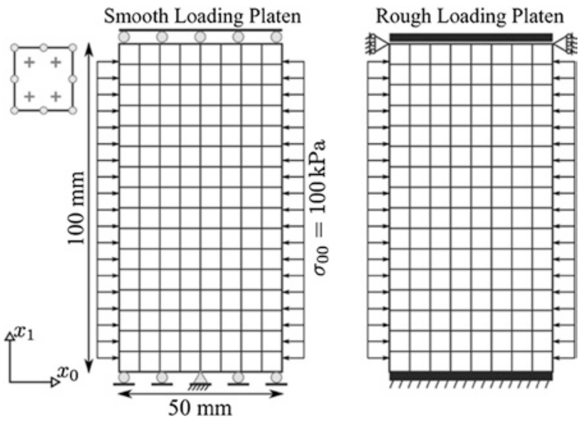

3 Results and Discussion

We demonstrate the predictive capacity of the hybrid FEM/DEM model described above by using it to simulate a biaxial compression test. Particular focus is placed here on the initiation and development of strain localization and the influence of boundary condition. The specimen has a dimension of 50 mm in width and 100 mm in height. First, it is discretized into a FEM mesh with 8×16 quadrilateral elements. We use the 8-node serendipity element with 4 Gauss integration point each. In total, 512 RVEs are used for the whole domain and they all possess the same initial condition, which leads to a uniform sample. Drained condition is imposed to the specimen, by maintaining a constant lateral confining pressure (i.e. $\sigma_{00} = 100\,\text{kPa}$) during the compression. The FEM mesh with quadrilateral element and the boundary conditions for the specimen are shown in Fig. 1.

The resultant normal stresses on the loading platen are shown in Fig. 2 for both cases of boundary conditions. The result from a pure DEM test on the RVE is also

Fig. 2 Resultant normal stress on the loading platen during the compression tests

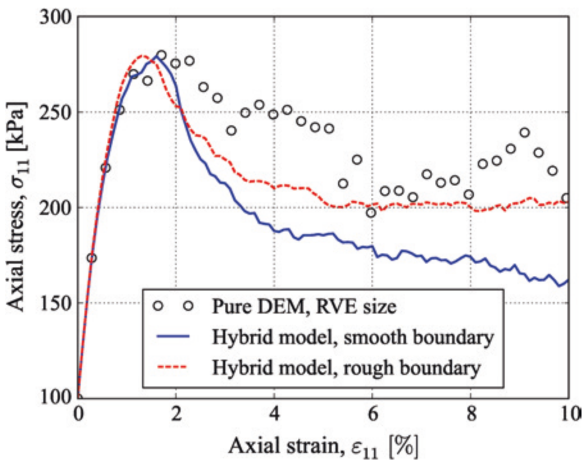

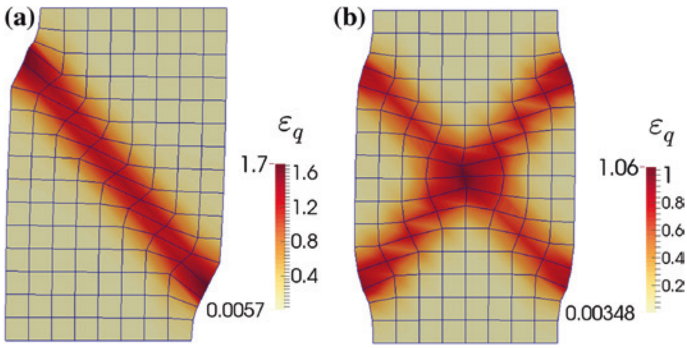

Fig. 3 Accumulated deviatoric strain contour showing strain localization: **a** *smooth* boundary; **b** *rough* boundary

presented for comparison. As seen from the figure, the hybrid model successfully predicts the typical response of dense sand subject to the biaxial compression as observed in laboratory and other conventional FEM simulations. For the smooth boundary case, the pre-peak response from the hybrid model matches the pure DEM test very well, while its post-peak response is much softer than that from the pure DEM test, which is attributable to the global strain localization as to be discussed later. For the rough boundary case, the initial stiffness is slightly higher than that in the smooth boundary condition due to the deformation of the specimen is restricted by the rough loading platen. The residual stress in this case (200 kPa) is also higher than that in the smooth case (160 kPa). However, the specimen attains almost the same peak strength in both cases (around 280 kPa).

The accumulated deviatoric strain contours at the final state (i.e. $\varepsilon_{11} = 10\,\%$) are presented in Fig. 3 which clearly shows that strain localization occurs in both cases. For the smooth boundary condition, a dominant single shear band is observed, while in the case using rough boundary, a pattern with crossed double shear bands is observed. These observations are consistent with the results presented by Gao and Zhao (2013) and the laboratory tests by Tatsuoka et al. (1990). Note that as the specimen is initially uniform and the loading condition is symmetric, no strain localization can be predicted by most conventional models when smooth boundary is used in conventional FEM tests, due to the lacking of symmetry breaker. Many studies have introduced artificial imperfections or random fields in order to trigger strain localization. While in the current hybrid model, the material response is captured by the RVE which is disordered and contains inherent heterogeneity in nature. This heterogeneity, though considerably small when the RVE is prepared to be isotropic, leads to a non-coaxial behavior of the granular media which initiate the strain localization (c.f. Gao and Zhao 2013).

4 Conclusions

We present a study on the strain localization in biaxial compression tests with a novel hybrid FEM/DEM approach. This modeling technique successfully reproduces the granular media responses without introducing any phenomenological constitutive relation for FEM. The influences of boundary conditions are examined. The use of rough loading platen results in a stiffer response than the use of a smooth one. And with a smooth boundary condition, only one dominant single shear band is developed; while in the case of rough boundary condition, two crossed shear bands are seen in the initially uniform specimen. Further microscopic studies are required to reveal the underlying mechanisms of the initiation of shear band in granular media.

Acknowledgments This work was supported by RGC HK (Grant No. 623609).

References

Fu P, Dafalias YF (2011) Fabric evolution within shear bands of granular materials and its relation to critical state theory. Int J Numer Anal Meth Geomech 35:1918–1948
Gao Z, Zhao J (2013) Strain localization and fabric evolution in sand. Int J Solids Struct 50:3634–3648
Gross L, Bourgouin L, Hale A, Muhlhaus H (2007) Interface modelling in incompressible media using level sets in escript. Phys Earth Planet Inter 163:23–34
Guo N, Zhao J (2013) A hierarchical model for cross-scale simulation of granular media. AIP Conf Proc 1542:1222–1225
Ishihara K, Oda M (1998) Rolling resistance at contacts in simulation of shear band development by DEM. J Eng Mech 124:285–292
Kruyt N, Rothenburg L (1998) Statistical theories for the elastic moduli of two-dimensional assemblies of granular materials. Int J Eng Sci 36:1127–1142
Šmilauer V, Catalano E, Chareyre B, Dorofeenko S, Duriez J, Gladky A, Kozicki J, Modenese C, Scholtès L, Sibille L, Stránský J, Thoeni K (2010) Yade reference documentation. The Yade Project
Tatsuoka F, Nakamura S, Huang CC, Tani K (1990) Strength anisotropy and shear band direction in plane strain tests of sand. Soils Found 30:35–54
Tejchman J, Wu W (2009) Non-coaxiality and stress-dilatancy rule in granular materials: FE investigation within micro-polar hypoplasticity. Int J Numer Anal Meth Geomech 33:117–142